

Effect of cerium oxide nanoparticles on the antimicrobial properties and retentive strength of glass ionomer cement for orthodontic band cementation

Hooman Shafaei^{1,2}, Khashayar Mohsenzadeh³, Hamidreza Rahimi⁴, Kiarash Ghazvini⁵, Abdolrasoul Rangrazi^{6*}

Abstract

Objective: This study aimed to investigate the antimicrobial effects and retentive strength of glass ionomer cement (GIC) containing cerium oxide nanoparticles (NPs) when used for cementing orthodontic bands, as well as to evaluate the cytotoxicity of these nanoparticles.

Methods: Cerium oxide nanoparticles (NPs) were incorporated into glass ionomer cement (GIC) at concentrations of 1%, 2%, and 4%. Disc-shaped specimens were prepared for each concentration, along with a control group without nanoparticles. Antibacterial activity was evaluated against *Streptococcus mutans* using the direct contact test. The lowest concentration of cerium oxide NPs that thoroughly eliminated bacterial growth was identified and then compared with the control group in the retentive strength test. In addition, cytotoxicity of cerium oxide NPs was assessed on gingival fibroblast cells using the MTT assay. The difference in retentive strength between the two groups was evaluated using an independent samples t-test at the significance level of $P < 0.05$.

Results: The direct contact test showed that a 1 wt% concentration of cerium oxide NPs was sufficient to eliminate all *Streptococcus mutans*. Incorporating 1 wt% cerium oxide into GIC did not significantly affect its retentive strength ($P = 0.31$). Cytotoxicity testing indicated that cerium oxide NPs have relatively low toxicity, with an IC_{50} (half maximal inhibitory concentration) value of 1000 $\mu\text{g/mL}$.

Conclusions: GIC containing 1 wt% cerium oxide NPs demonstrated significant antibacterial activity against *Streptococcus mutans*, maintained acceptable retentive strength, and exhibited relatively low cytotoxicity.

Keywords: Anti-bacterial agents, Cerium, Glass ionomer cements, Nanoparticles, Orthodontic appliances, *Streptococcus mutans*

Introduction

Fixed orthodontic treatment plays an important role in achieving proper tooth alignment and improving both dental esthetics and the function of the masticatory system (1). However, fixed appliances can increase dental plaque accumulation because the rough surfaces of brackets, bands, and wires interfere with natural self-

cleaning mechanisms and make effective tooth brushing more difficult (2-4).

To reduce the risk of caries during orthodontic treatment, primary preventive measures such as maintaining good oral hygiene and limiting sugar intake are recommended, along with secondary approaches such as fluoride application. However, these preventive measures are often unreliable because they rely heavily on patient compliance (5). An alternative approach is to incorporate antibacterial nanoparticles into composite resins, adhesives, or cement to provide antimicrobial effects (6, 7).

Orthodontic bands are typically placed on molars and remain cemented in position throughout treatment (8). White spot lesions resulting from decalcification are frequently observed around banded teeth after completion of orthodontic treatment. These lesions are attributed to an increased number of plaque-retentive areas and reduced efficiency of mechanical plaque removal following band placement (9, 10). Another

¹Dental Materials Research Center, Mashhad University of Medical Sciences, Mashhad, Iran

²Department of Orthodontics, School of Dentistry, Mashhad University of Medical Sciences, Mashhad, Iran

³School of Dentistry, Mashhad University of Medical Sciences, Mashhad, Iran

⁴Medical Genetics and Molecular Medicine, School of Medicine, Mashhad University of Medical Sciences, Mashhad, Iran

⁵Antimicrobial Resistance Research Center, Mashhad University of Medical Sciences, Mashhad, Iran

⁶Dental Research Center, Mashhad University of Medical Sciences, Mashhad, Iran

*Corresponding Author: Abdolrasoul Rangrazi
Email: rangrazi.r@gmail.com

Accepted: 9 February 2026. Submitted: 17 November 2025



important factor that can promote caries is microleakage at the interface between the tooth, cement, and band. Microleakage allows bacteria and oral fluids to penetrate beneath the band, increasing the risk of enamel demineralization and white spot lesion formation (11). Therefore, orthodontic band cements should provide a good seal, reduce plaque accumulation, and maintain adequate mechanical strength (12).

The application of nanotechnology in orthodontics shows considerable promise and has been extensively studied. Nanotechnology can enhance the performance of fixed orthodontic appliances by reducing friction, inhibiting bacterial growth, promoting tooth remineralization, improving corrosion resistance and biocompatibility of metal components, and facilitating orthodontic tooth movement (13). Various nanoparticles, such as silver (Ag), titanium dioxide (TiO₂), silver–hydroxyapatite (Ag-HA), curcumin, zirconia–titania (ZrO₂-TiO₂), copper oxide (CuO), zinc oxide (ZnO), cinnamon extract, magnesium oxide (MgO), and chitosan have been incorporated into GIC or orthodontic composites to enhance antibacterial or mechanical properties for banding or bonding in fixed orthodontic treatment (5-7).

Cerium oxide (CeO₂) nanoparticles (NPs) have attracted attention for biomedical applications due to their antioxidant, anti-inflammatory, angiogenic, and antibacterial properties (14). Cerium oxide has demonstrated strong antibacterial activity against a wide range of gram-positive and gram-negative bacteria (15). These nanoparticles can be potentially applied to enhance the antibacterial properties of GIC used for orthodontic bands, thus improving its caries-preventive potential. However, any modification of GIC with CeO₂ must be carefully evaluated to ensure that it does not adversely affect the retentive strength of orthodontic bands.

To the best of our knowledge, no previous study has investigated the effect of cerium oxide nanoparticles on antimicrobial and mechanical properties of luting cements. Therefore, the present study aimed to investigate the antimicrobial effects and retentive strength of glass ionomer cement (GIC) containing cerium oxide nanoparticles (NPs) when used for cementing orthodontic bands, as well as to evaluate the cytotoxicity of these nanoparticles.

Materials and methods

Study design and ethical consideration

This in vitro study was conducted in the Dental Materials Laboratory at the School of Dentistry, Mashhad University of Medical Sciences, Mashhad, Iran. All procedures were performed in accordance with the principles of the Declaration of Helsinki and were approved by the ethics committee of Mashhad University of Medical Sciences (Ethics code: IR.MUMS.DENTISTRY.REC.1401.142).

Sample size calculation

Based on the study by Heravi et al. (16) and the reported mean values and standard deviations of retentive strength, the sample size was calculated using G*Power 3.1 software with $\alpha = 0.05$, $\beta = 0.05$, and an effect size of 1.34, resulting in 15 samples per group for retentive strength assessment. For the antibacterial tests and MTT cytotoxicity assay, where significant variability was not anticipated, three samples per group were included (6, 7).

Synthesis of cerium oxide NPs

First, solutions of cerium nitrate hexahydrate (Ce(NO₃)₃·6H₂O; Merck, Darmstadt, Germany) and sodium hydroxide (NaOH; Merck) were prepared separately in two 250 mL beakers. The cerium nitrate hexahydrate solution was placed on a magnetic stirrer, and the sodium hydroxide solution was added dropwise and gradually to it. The resulting suspension was centrifuged at 8000 rpm for 15 minutes to collect the precipitate. The supernatant was discarded, and the precipitate was washed several times with water. Finally, the precipitate was dried in a vacuum oven at 200 °C, yielding cerium oxide nanoparticle powder (17). X-ray diffraction (XRD) (GNR, Italy) and transmission electron microscopy (TEM) (Leo 912 AB, Carl Zeiss, Oberkochen, Germany) tests were performed on the synthesized cerium oxide NPs.

Figure 1 shows the XRD pattern of the synthesized cerium oxide NPs. The sharp, well-defined diffraction peaks correspond to the characteristic reflections of cerium oxide with a cubic fluorite-type structure, confirming a highly crystalline and single-phase material (18).

Figure 2 shows the TEM image and particle size distribution of the synthesized cerium oxide NPs. The average particle size was 16.1 ± 3.55 nm.

Incorporation of cerium oxide NPs into luting cement

Cerium oxide NPs were incorporated into GIC powder at concentrations of 1%, 2%, and 4% using a dry-mixing

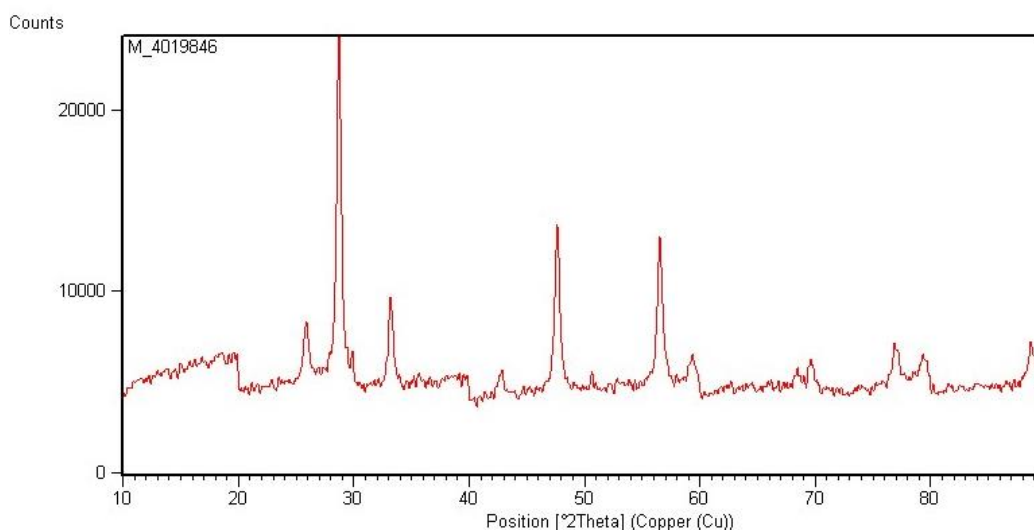


Figure 1. The x-ray diffraction (XRD) pattern for cerium oxide nanoparticles

method. Briefly, the required amounts of cerium oxide nanoparticles were accurately weighed and then gradually added to the pre-measured GIC powder. The mixture was then thoroughly blended manually using a spatula to achieve a uniform distribution of the nanoparticles and minimize agglomeration.

Antibacterial activity assessment

The antibacterial activity of GIC containing cerium oxide NPs was evaluated against *Streptococcus mutans* (*S. mutans*) using a direct contact test, adapted from ISO 22196 and previously published protocols (7). Cerium oxide NPs powder was incorporated into a luting and lining GIC (GC Corporation, Tokyo, Japan) at concentrations of 1%, 2%, and 4% by weight (wt%).

After mixing the powder and liquid components (powder/liquid ratio = 1.4:1, g/g), the mixture was placed into a custom-made Teflon mold to produce disk-shaped specimens (15 mm in diameter and 2 mm in height). Three disks were prepared for each concentration, and control disks without nanoparticles were fabricated using the same procedure. All specimens were allowed to set completely according to the manufacturer's instructions.

The antibacterial activity test was conducted following the protocol outlined below. *S. mutans* were obtained from the Persian Type Culture Collection of the Scientific and Industrial Research Center of Iran under the bacterial number PTCC No: 1683 (equivalent to ATCC 35668). *S. mutans* was revived from its lyophilized form and transferred from the stock culture to fresh culture medium, where it was incubated for 24 hours. The surfaces to be tested were placed in sterile plates and decontaminated using direct and near-ultraviolet radiation for 60 minutes.

Bacteria were cultured in Brain Heart Infusion Broth and allowed to grow for 4–5 hours until the turbidity of the medium reached half McFarland turbidity. This standard turbidity was then diluted to achieve a bacterial cell concentration of 1×10^5 CFU/mL per 100 μ L. This solution was used as the inoculation suspension for the test surfaces.

To examine the external surface of the prepared specimens, each sample was placed in a separate sterile

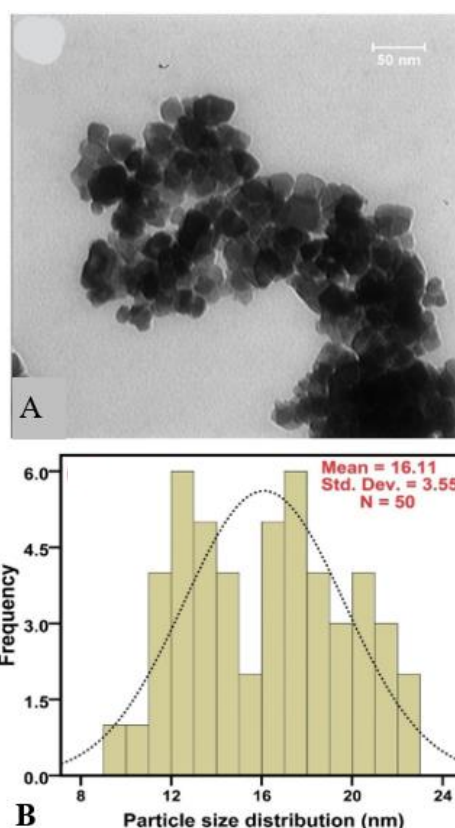


Figure 2. (A) A transmission electron microscopy (TEM) graph of cerium oxide (CeO_2) nanoparticles (NPs); (B) The size distribution of CeO_2 NPs

plate. Then, 100 μL of diluted bacterial suspension was added to each surface. Two inoculation sites were performed on each specimen: one for baseline measurement (time zero) and the other for post-exposure evaluation. A clean laboratory slide was used as the negative control.

The inoculated surfaces were incubated for 1 hour at room temperature. Afterward, they were washed with liquid culture medium, and the wash was transferred to blood agar culture plates, which were then incubated for 48 hours. The culture results were evaluated after 48 hours of incubation, the cultures were evaluated, and the bacterial load was quantified. The minimum proportion of cerium oxide nanoparticles required to kill all bacteria was compared to the control group in the next step of evaluating its retentive strength.

Retentive strength test

The retentive strength of GIC containing the minimum effective concentration of cerium oxide NPs was evaluated and compared with that of the control group.

Thirty extracted premolars were selected based on specific inclusion criteria, including the absence of caries, restorations, cracks, or surface defects. The root of each tooth was embedded in a plastic model and fixed with cold-cure acrylic resin (Acropars, Tehran, Iran). The teeth were subsequently cleaned with a pumice slurry, rinsed with distilled water, and air-dried. Each tooth was coded and randomly assigned to one of the two groups using a random numbers table ($n = 15$). The grouping

was based on the material used for band cementation, as follows:

- Control group: cementation with conventional GIC.
- Experimental group: cementation with GIC containing 1 wt% cerium oxide NPs.

For each tooth, an appropriately sized stainless steel orthodontic band (Dentaurum, Pforzheim, Germany) was selected by a single experienced orthodontist. Band selection aimed to achieve a tight fit, with complete seating of the cervical margin at the cemento-enamel junction (CEJ) and no visible gaps, rocking, or deformation. Bands that did not meet these criteria were replaced with the next suitable size to ensure a consistent fit across all specimens.

To minimize variations in cement film thickness, a single operator mixed the glass ionomer luting and lining cement according to the manufacturer's instructions (powder/liquid ratio = 1.4:1 g/g). A standardized thin layer of cement was applied to the inner surface of each band using a small spatula, ensuring complete coverage without overfilling. Each band was then positioned on the tooth and seated with firm, steady finger pressure for approximately 30 seconds. Excess cement extruded at the margins was carefully removed with a cotton roll before setting. This procedure was applied consistently to all specimens.

For the retentive strength test, a custom-made device (Figure 3) was used to apply force to the bands. The tool, consisting of 13 components, was positioned under the buccal and lingual arms of each band and connected to the load cell of the testing apparatus. Its design allowed

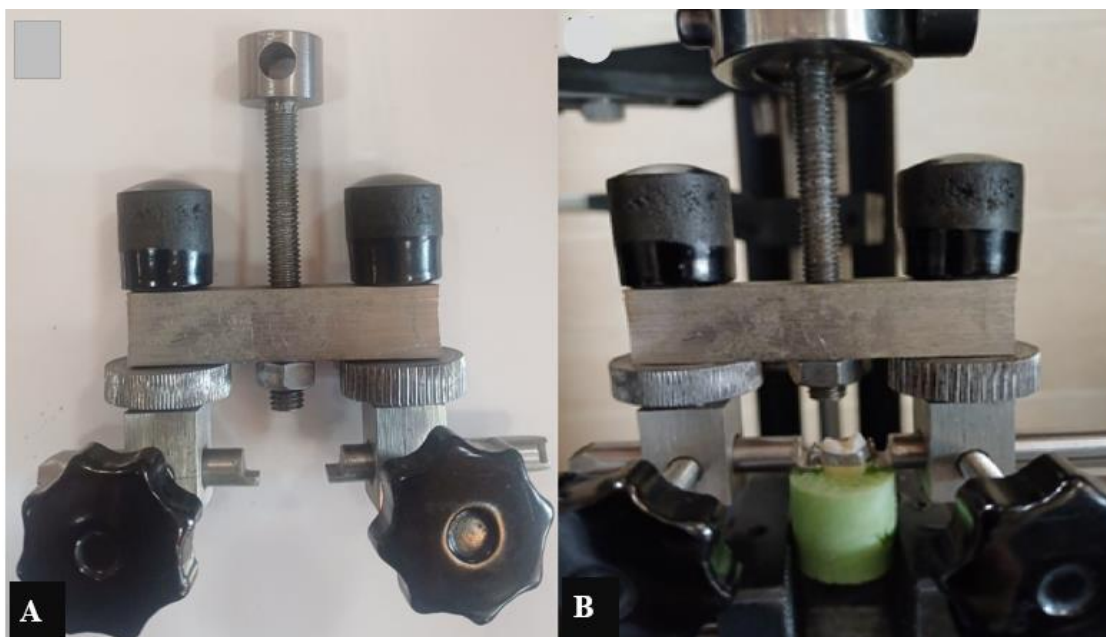


Figure 3. (A) A customized band removal device for assessing retentive strength; (B) Placement of a sample in the universal testing machine for the retentive strength test

precise horizontal and vertical adjustment of each arm, ensuring accurate and reproducible force application (Figure 3A). The lingual sheath was welded to each orthodontic band to ensure stable attachment.

The retentive strength of cement was measured by a universal testing machine (STM20; SANTAM, Tehran, Iran). Each tooth sample was secured in the machine's clamp. The arrowheads of the holding device were fully engaged beneath both the bracket and the lingual sheath of each band, ensuring stable positioning. The Force was applied at a crosshead speed of 1 mm/min until the band detached from the tooth (Figure 3B).

The force required to separate each band was recorded in Newtons and then divided by the area of the respective band (in mm²) to calculate the retentive strength (in megapascals).

Cytotoxicity assessment

Cytotoxicity of cerium oxide NPs was assessed by the MTT assay. To prepare the MTT solution, 5 mg of MTT powder was dissolved in 1 mL of sterile phosphate-buffered saline (PBS). The MTT solution is normally yellow in color. However, in the presence of viable cells, mitochondrial enzymes reduce MTT to insoluble purple formazan crystals. Therefore, the intensity of the purple color formed is directly related to the number of living, metabolically active cells.

Following cell counting, 2×10^3 gingival fibroblast cells (Pasteur Institute, Tehran, Iran) were seeded into each well of a 96-well plate. After 24 hours, allowing sufficient time for cell attachment, the cells were treated with different concentrations of cerium oxide NPs, starting from an initial concentration of 1.4 mg/mL. For the treatment groups, 100 μ L of nanoparticle suspension at the desired concentrations was added to each well. In the control group, 100 μ L of culture medium containing fetal bovine serum (FBS) was added instead. The cells were then incubated for 48 hours.

After the incubation period, the culture medium was carefully removed from each well, and the wells were gently washed with PBS. Next, 20 μ L of MTT solution (5 mg/mL) was added to each well under sterile conditions and protected from light. The plate was incubated for an

additional 4 hours to allow the formation of formazan crystals. Following this step, the supernatant was removed, and 100 μ L of dimethyl sulfoxide (DMSO) was added to each well to dissolve the purple crystals. The plate was then shaken for 15 minutes to ensure complete dissolution.

Finally, the optical density (OD) of each well was measured at 570 nm, using 630 nm as a reference wavelength. All experiments were performed in triplicate to ensure accuracy and reproducibility. For data analysis, the absorbance at 630 nm was subtracted from the absorbance at 570 nm to correct for background interference. These corrected values were then compared with the control group. A dose–response curve was generated using appropriate software, and the half-maximal inhibitory concentration (IC₅₀) of the test compound was determined.

Statistical analysis

The normality of retentive strength data was assessed using the Kolmogorov–Smirnov test ($P > 0.05$). The difference in retentive strength between the two groups was evaluated using an independent samples t-test. The data were analyzed using IBM SPSS Statistics software (version 25.0; IBM Corp., Armonk, NY, USA), and the statistical significance was set at $P < 0.05$.

Results

Antibacterial activity assessment

The direct contact test results indicated that the control GIC group had 160 ± 26 CFU/mL of *S. mutans*, whereas all cerium oxide-containing groups (1 wt%, 2 wt%, and 4 wt%) showed complete bacterial inhibition (0 CFU/mL). The 1 wt% cerium oxide was the lowest concentration required to achieve full elimination of *S. mutans* (Table 1).

Retentive strength test

Based on the antimicrobial test results, the GIC containing 1% cerium oxide NPs was selected for the retentive strength evaluation and compared with the control group. Table 2 presents the mean and standard

Table 1. Antimicrobial test results of GIC containing cerium oxide nanoparticles against *Streptococcus mutans*

Groups	CFU/ml
	Mean \pm SD
Glass ionomer cement (Control)	160 \pm 26
Glass ionomer cement + 1% cerium oxide nanoparticles	0
Glass ionomer cement + 2% cerium oxide nanoparticles	0
Glass ionomer cement + 4% cerium oxide nanoparticles	0

CFU: colony-forming units

Table 2. Mean and standard deviation of the retentive strength of bands in the study groups

Groups	Mean (MPa)	Standard Deviation
Glass ionomer (Control)	0.5825	0.1233
Glass ionomer containing 1% CeO ₂ NPs	0.5366	0.1194
P-value*	0.31	

*independent samples t-test

CeO₂ NPs: Cerium oxide nanoparticles

deviation of retentive strength for both groups. An independent samples t-test indicated no significant difference in retentive strength between the groups (P = 0.31).

Cytotoxicity assessment

Figure 4 presents the results of the cytotoxicity assay of cerium oxide NPs on gingival fibroblast cells, showing cell viability at different nanoparticle concentrations.

The results indicated that the IC₅₀, the concentration required to inhibit the growth of 50% of cells, was 1000 µg/mL for cerium oxide nanoparticles.

Discussion

In this study, the antibacterial activity of GIC containing various concentrations of cerium oxide (CeO₂) nanoparticles (NPs) was assessed using the direct contact test, and the minimum concentration of cerium oxide NPs required to inhibit *S. mutans* was determined. GIC containing this minimum concentration (1% w/w) was then compared with control GI cement (without nanoparticles) in the retentive strength test. Finally, the cytotoxicity of cerium oxide NPs was evaluated on gingival fibroblast cells. Cerium oxide NPs were considered suitable for this study due to their reported activity against a broad spectrum of both gram-positive and gram-negative bacteria (15).

In the present study, all cerium oxide-containing groups (1 wt%, 2 wt%, and 4 wt%) showed complete bacterial inhibition (0 CFU/mL). Therefore, even the

lowest concentration tested was sufficient to achieve complete bacterial elimination under the experimental conditions. Furthermore, the minimum bactericidal threshold is ≤ 1 wt%, since increasing the concentration did not produce a measurable additional reduction.

Although the antibacterial mechanism of cerium oxide NPs is not fully understood, two main mechanisms of action have been proposed. In the direct mechanism, cerium oxide NPs physically interact with the bacterial cell wall and membrane. This interaction leads to the production of reactive oxygen species (ROS), such as hydrogen peroxide, which damage the cell. The damage is largely localized and contact-dependent, often resulting in membrane breakdown and cell lysis. In the indirect mechanism, cerium oxide NPs nanoparticles primarily interact with the surrounding environment or extracellular components, such as the polysaccharide-rich outer layers of the bacterial cell wall. This interaction promotes the generation of ROS outside the cell. These ROS then diffuse or penetrate the bacterial cell. Inside the cell, they cause secondary damage to intracellular targets, including proteins, enzymes, and DNA, ultimately leading to cell death.

The outcomes of this study are in agreement with the results of Pop et al (19), who demonstrated that cerium oxide NPs exhibit significant antibacterial effects against *Escherichia coli*, *Salmonella typhimurium*, *Listeria monocytogenes*, *Staphylococcus aureus*, and *Bacillus cereus*. Bhatt et al. (20) also investigated the potential of cerium oxide NPs to reduce dental caries. In an in vitro

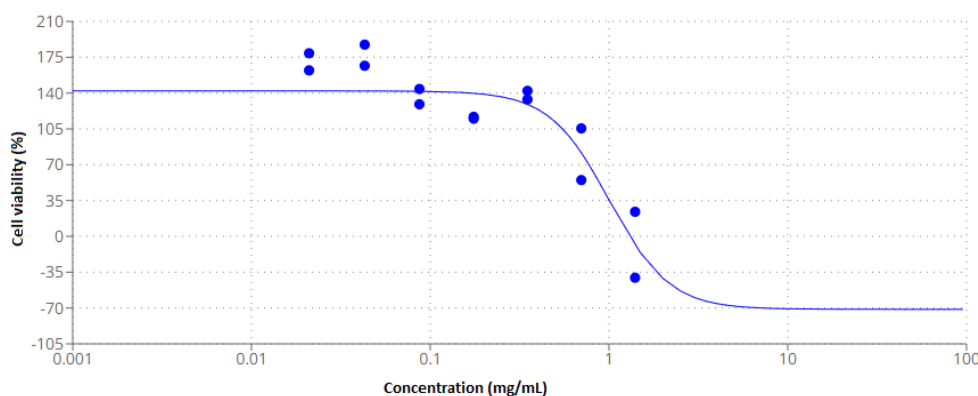


Figure 4. A graph depicting the percentage of cell viability of gingival fibroblasts at different concentrations of cerium oxide nanoparticles

model of initial *S. mutans* colonization, cerium oxide NPs reduced bacterial adhesion by approximately 40%, suggesting a potential decrease in caries risk. The outcomes of this study are in contrast to those of Jairam et al. (21), who incorporated cerium oxide nanoparticles at different concentrations into restorative glass ionomer cement and assessed their antibacterial activity against *Streptococcus mutans* using the agar well diffusion method. They found that the antibacterial activity of the cement increased with the addition of cerium oxide NPs up to 4%, but decreased at higher concentrations. This reduction was attributed to nanoparticle agglomeration, which diminishes the active surface area of the cerium oxide NPs. These different results could be attributed to the method of antibacterial activity assessment and the type of GIC employed.

In the present study, the 1 wt% cerium oxide was the lowest concentration required to achieve full elimination of *S. mutans*, and thus this ratio was selected for retentive strength measurement. The results indicated no significant difference in the retentive strength between the GIC containing 1% cerium oxide and the control group. This finding implies that incorporating 1% cerium oxide NPs into GIC does not adversely affect its retentive strength. A review of the literature shows no previous study that examined the retentive strength of bands cemented with GIC containing cerium oxide. Heravi et al. (22) reported that modifying GIC with 1.56% w/w CPP-ACP did not reduce the retentive strength of bands. Similarly, Hatunoğlu et al. (23) found that adding 10%, 25%, or 50% ethanolic extracts of propolis (EEP) to conventional GIC did not adversely affect the shear-peel band strength.

The widespread use of cerium oxide NPs has raised concerns about their potential effects on human health. Nanomaterials are much smaller than cells, allowing them to penetrate cell membranes and interact with intracellular organelles. This may lead to adverse effects such as neurotoxicity, immunotoxicity, and genotoxicity. The cytotoxicity of metal nanoparticles is influenced by several factors, including their composition, size, shape, surface charge, solubility, and chemical reactivity (24).

In this study, the cytotoxicity of cerium oxide NPs was assessed on gingival fibroblast cells. The results indicated that the IC_{50} , the concentration required to inhibit the growth of 50% of cells, was 1000 $\mu\text{g}/\text{mL}$ for cerium oxide NPs. In comparison, Shafaei et al. (6) reported IC_{50} values of 1060 $\mu\text{g}/\text{mL}$ for cinnamon NPs, 460 $\mu\text{g}/\text{mL}$ for zinc oxide NPs, and 380 $\mu\text{g}/\text{mL}$ for copper oxide NPs. The IC_{50} of 1000 $\mu\text{g}/\text{mL}$ for cerium oxide NPs

indicates lower cytotoxicity than zinc oxide and copper oxide NPs, and a cytotoxicity level similar to that of cinnamon NPs. Kim et al (25) found that the overall toxicity of cerium oxide NPs was considerably lower than that of zinc oxide NPs, which are widely used in dental research. Interestingly, cerium oxide NPs have been reported to play a protective role against nitric oxide-induced toxicity. Akhtar et al. (26) observed that cerium oxide NPs at 100 $\mu\text{g}/\text{mL}$ mitigated nitric oxide-induced toxicity in endothelial cells. Bhatt et al. (20) reported only minor effects on human cell metabolism at concentrations up to 1 mM cerium and noted that cerium oxide NPs exhibited lower cytotoxicity than equimolar silver nitrate (AgNO_3).

In contrast, several studies showed that cerium oxide NPs can induce reactive oxygen species (ROS) production, DNA damage, cell death, and apoptosis in human lung cells (27-29). Cytotoxic and oxidative effects of cerium oxide NPs have also been reported in human skin keratinocytes, along with genotoxicity in human intestinal Caco-2 cells (30-32). Benameur et al. (33) observed that low concentrations of cerium oxide nanoparticles (6 $\mu\text{g}/\text{mL}$ and 6 mg/mL) caused genetic damage and oxidative stress in dermal fibroblast cells, with chromosomal damage and DNA structural alterations identified as primary mechanisms of toxicity.

The main limitation of this study is that it was conducted in vitro using extracted human premolars and gingival fibroblast cultures. Therefore, the results cannot fully replicate the complex biological, microbiological, and mechanical environment of the oral cavity. Additionally, antibacterial activity was assessed against a single bacterial species (*S. mutans*) over a short incubation period, and cytotoxicity was evaluated in a single cell line using the MTT assay. Future studies should employ in vitro or in vivo models that better mimic oral conditions, extend antibacterial testing to multispecies biofilms and additional cariogenic or periodontal pathogens, and assess cytotoxicity across multiple cell types using complementary assays, ultimately progressing toward well-designed clinical trials.

Conclusions

1. The minimum concentration of cerium oxide nanoparticles required to completely inhibit *S. mutans* was determined to be 1% by weight.
2. Incorporating 1% cerium oxide nanoparticles into GIC did not significantly affect its retentive strength for band cementation, indicating that this

concentration preserves the material's suitability for orthodontic applications.

- The IC_{50} of cerium oxide nanoparticles was 1000 $\mu\text{g/mL}$, suggesting relatively low cytotoxicity toward gingival fibroblast cells.

Acknowledgments

None

Conflict of interest

The authors declare that they have no conflict of interest.

Author contributions

A.R. and H.S. developed the project, supervised the study, obtained funding, helped in data analysis, and edited the manuscript. K.G. supervised the study, helped in data analysis, and edited the manuscript. K.M. and H.R. collected the data and edited the manuscript. All authors read and approved the final manuscript.

Ethical considerations

The protocol of the present study was approved by the Research Ethics Committee of Mashhad University of Medical Sciences (IR.MUMS.DENTISTRY.REC.1401.142).

Funding

This research was funded by the vice chancellor for research at Mashhad University of Medical Sciences (Grant number: 4011807).

References

- Yetkiner E, Dogan E, Güner G. Influence of different bonding agents on the color stability of enamel after orthodontic bracket removal. *J Dent Mater Tech* 2024;13(1):38–43.
- Salerno C, Grazia Cagetti M, Cirio S, Esteves-Oliveira M, Wierichs RJ, Kloukos D, et al. Distribution of initial caries lesions in relation to fixed orthodontic therapy. A systematic review and meta-analysis. *Eur J Orthod* 2024;46(2):cjae008.
- Wisth P, Nord A. Caries experience in orthodontically treated individuals. *Angle Orthod* 1977;47(1):59–64.
- Merati M, Sabzevari B. Effects of a fluoride-releasing orthodontic cement on preventing the development of white spot lesions. *J Dent Mater Tech* 2024;13(2):60–65.
- Pourhajibagher M, Sodagar A, Bahador A. An in vitro evaluation of the effects of nanoparticles on shear bond strength and antimicrobial properties of orthodontic adhesives: A systematic review and meta-analysis study. *Int Orthod* 2020;18(2):203–213.

- Shafae H, Khosropanah H, Rahimi H, Darroudi M, Rangrazi A. Effects of adding cinnamon, ZnO, and CuO nanoparticles on the antibacterial properties of a glass ionomer cement as the luting agent for orthodontic bands and their cytotoxicity. *J Composites Sci* 2022;6(11):336.
- Rangrazi A, Daneshmand MS, Ghazvini K, Shafae H. Effects of magnesium oxide nanoparticles incorporation on shear bond strength and antibacterial activity of an orthodontic composite: an in vitro study. *Biomimetics* 2022;7(3):133.
- Bandeira AM, Martinez EF, Demasi APD. Evaluation of toxicity and response to oxidative stress generated by orthodontic bands in human gingival fibroblasts. *Angle Orthod* 2020;90(2):285–290.
- Prabha RD, Kandasamy R, Sivaraman US, Nandkumar MA, Nair PD. Antibacterial nanosilver coated orthodontic bands with potential implications in dentistry. *Indian J Med Res* 2016;144(4):580–586.
- Demling A, Elter C, Heidenblut T, Bach F-W, Hahn A, Schwestka-Polly R, et al. Reduction of biofilm on orthodontic brackets with the use of a polytetrafluoroethylene coating. *Eur J Orthod* 2010;32(4):414–418.
- Gillgrass T, Millett D, Creanor S, MacKenzie D, Bagg J, Gilmour W, et al. Fluoride release, microbial inhibition and microleakage pattern of two orthodontic band cements. *J Dent* 1999;27(6):455–461.
- Sande FHvd, Silva AFd, Michelon D, Piva E, Cenci MS, Demarco FF. Surface roughness of orthodontic band cements with different compositions. *J Appl Oral Sci* 2011;19:223–227.
- He L, Zhang W, Liu J, Pan Y, Li S, Xie Y. Applications of nanotechnology in orthodontics: a comprehensive review of tooth movement, antibacterial properties, friction reduction, and corrosion resistance. *Biomed Eng Online* 2024;23(1):72.
- Nosrati H, Heydari M, Khodaei M. Cerium oxide nanoparticles: synthesis methods and applications in wound healing. *Mater Today Bio* 2023;23:100823.
- Zhang M, Zhang C, Zhai X, Luo F, Du Y, Yan C. Antibacterial mechanism and activity of cerium oxide nanoparticles. *Sci China Mater* 2019;62(11):1727–1739.
- Heravi F, Omidkhoda M, Koohestanian N, Hooshmand T, Bagheri H, Ghaffari N. Retentive strength of orthodontic bands cemented with amorphous calcium phosphate-modified glass ionomer cement: an in-vitro study. *J Dent* 2017;14(1):13.
- Tumkur PP, Gunasekaran NK, Lamani BR, Nazario Bayon N, Prabhakaran K, Hall JC, et al. Cerium oxide nanoparticles: synthesis and characterization for biosafe applications. *Nanomanufacturing* 2021;1(3):176–189.
- Ioannou ME, Pouroutzidou GK, Chatzimentor I, Tsamesidis I, Florini N, Tsiaoussis I, et al. Synthesis and characterization of cerium oxide nanoparticles: effect of cerium precursor to gelatin ratio. *Appl Sci* 2023;13(4):2676.
- Pop OL, Mesaros A, Vodnar DC, Suharoschi R, Tăbăran F, Mageruşan L, et al. Cerium oxide

nanoparticles and their efficient antibacterial application in vitro against gram-positive and gram-negative pathogens. *Nanomaterials* 2020;10(8):1614.

20. Bhatt L, Chen L, Guo J, Klie RF, Shi J, Pesavento RP. Hydrolyzed Ce (IV) salts limit sucrose-dependent biofilm formation by *Streptococcus mutans*. *J Inorg Biochem* 2020;206:110997.

21. Jairam LS, Chandrashekar A, Prabhu TN, Kotha SB, Girish M, Devraj IM, et al. A review on biomedical and dental applications of cerium oxide nanoparticles—unearthing the potential of this rare earth metal. *J Rare Earths* 2023;41(11):1645–1661.

22. Heravi F, Bagheri H, Rangrazi A, Zebarjad SM. An in vitro study on the retentive strength of orthodontic bands cemented with CPP-ACP-containing GIC. *Mater Res Express* 2016;3(12):125401.

23. Hatunoğlu E, Öztürk F, Bilenler T, Aksakallı S, Şimşek N. Antibacterial and mechanical properties of propolis added to glass ionomer cement. *Angle Orthod* 2014;84(2):368–373.

24. Xiong P, Huang X, Ye N, Lu Q, Zhang G, Peng S, et al. Cytotoxicity of metal-based nanoparticles: from mechanisms and methods of evaluation to pathological manifestations. *Adv Sci (Weinh)* 2022;9(16):2106049.

25. Kim I-S, Baek M, Choi S-J. Comparative cytotoxicity of Al₂O₃, CeO₂, TiO₂ and ZnO nanoparticles to human lung cells. *J Nanosci Nanotechnol* 2010;10(5):3453–3458.

26. Akhtar MJ, Ahamed M, Alhadlaq H. Anti-inflammatory CeO₂ nanoparticles prevented cytotoxicity due to exogenous nitric oxide donors via induction rather than inhibition of superoxide/nitric oxide in huve cells. *Molecules* 2021;26(17):5416.

27. Lin W, Huang Y-w, Zhou X-D, Ma Y. Toxicity of cerium oxide nanoparticles in human lung cancer cells. *Int J Toxicol* 2006;25(6):451–457.

28. Mittal S, Pandey AK. Cerium oxide nanoparticles induced toxicity in human lung cells: role of ROS mediated DNA damage and apoptosis. *BioMed Res Int* 2014;2014(1):891934.

29. Ma Y, Li P, Zhao L, Liu J, Yu J, Huang Y, et al. Size-dependent cytotoxicity and reactive oxygen species of cerium oxide nanoparticles in human retinal pigment epithelia cells. *Int J Nanomedicine* 2021:5333–5341.

30. Cheng G, Guo W, Han L, Chen E, Kong L, Wang L, et al. Cerium oxide nanoparticles induce cytotoxicity in human hepatoma SMMC-7721 cells via oxidative stress and the activation of MAPK signaling pathways. *Toxicol in Vitro* 2013;27(3):1082–1088.

31. Ngoc LTN, Bui VKH, Moon J-Y, Lee Y-C. In-vitro cytotoxicity and oxidative stress induced by cerium aminoclay and cerium oxide nanoparticles in human skin keratinocyte cells. *J Nanosci Nanotechnol* 2019;19(10):6369–6375.

32. Fisichella M, Berenguer F, Steinmetz G, Auffan M, Rose J, Prat O. Toxicity evaluation of manufactured CeO₂ nanoparticles before and after alteration: combined physicochemical and whole-genome expression analysis in Caco-2 cells. *BMC Genomics* 2014;15:(1)700.

33. Benameur L, Auffan M, Cassien M, Liu W, Culcasi M, Rahmouni H, et al. DNA damage and oxidative stress induced by CeO₂ nanoparticles in human dermal fibroblasts: Evidence of a clastogenic effect as a mechanism of genotoxicity. *Nanotoxicology* 2015;9(6):696–705.